Supplement to „ Intensity correlation-based calibration of FRET" (by L. Bene et al.)

Glossary of symbols

α_0: "spectroscopic" α-factor determined with the conventional way, Eq. 2;

α: α-factor determined with the correlation-based quadratic equation, Eq. 9;

α_{cubic}: α-factor determined with the correlation-based cubic equation, Eq. 20;

ε_d, ε_a: molar decadic extinction coefficients, for donor (d) and acceptor (a);

B_d, B_a: number of labeled binding sites, for donor (d) and acceptor (a);

L_d, L_a: dye/protein labeling ratios, for donor (d) and acceptor (a);

I_1, I_2, I_3: intensities in the donor channel, in the channel of sensitized emission, and in the acceptor channel, respectively;

I_d: unquenched donor intensity of the FRET sample;

M_d, M_a: mean values of intensities I_1 and I_2 of the single-labeled samples, for donor (d) and acceptor (a);

E: FRET efficiency as determined by the combined donor quenching and sensitized emission in the FCET method;

S_1, S_2, S_3: spectral spillage factors determined from single-labeled samples, Eqs. 4s-6s;

A': primarily determined FRET-related quantity of the FCET method from which FRET efficiency E is calculated as E=A'/(α+A'), Eq. 10s;

d_0: second central moment, variance of the donor intensity of the single donor-labeled sample $I_{1, \text{donor only}}$, d_0=($I_{1,}$, I_1)$_{\text{donor only}}$;

d': second central moment, variance of the quenched donor intensity of the FRET sample I_1, d=(I_1, I_1);

d: second central moment, variance of the unquenched donor intensity of the FRET sample I_d, d=(I_d, I_d);

D: difference of central moments for unquenched and quenched donor intensities d and d', D=d-d';

(ξ, ψ): covariance of the ξ and ψ random variables;

p: covariance of I_1 and I_1A', (I_1, I_1A');

q: variance of I_1A', (I_1A', I_1A');

Q: quenching efficiency calculated from donor intensity, Eq. 16;

Q': quenching efficiency calculated from second moments of donor intensity, Eq. 17;

m: slope of linear trend line fitting the Q' vs. Q plot, Eq. 18;

b: intercept of linear trend line fitting the Q' vs. Q plot, Eq. 18;

d_a': second central moment of acceptor without FRET calculated from I_a, Eq. 29s;

d_a'': second central moment of acceptor with FRET calculated from I_a and I_1A', Eq. 30s;

p_i, i=0, 1, 2, 3: coefficient of the ith order term in the cubic equation for α_{cubic}, Eqs. 21-24;

CV_ξ: coefficient of variation for random variable ξ, $CV_\xi = \sqrt{(\xi, \xi)} / \overline{\xi}$, Eqs. 37s-39s, 53s-55s.

Organization of paper

As to the organization of the main text, in the *Theoretical results* part first a quadratic equation for α is deduced. Then its properties are discussed for sterically interacting and non-interacting (competing vs. non-competing) dye-targeting labels (mAbs). For competing labels estimation of the moment of the donor-only sample in the coefficient of the leading term quadratic in α is given based on: (i) Experimentally recorded modulation of variance (2nd moment) of donor intensity vs. mean intensity („Q'-Q plots"). (ii) Observed modulation of variance of donor intensity vs. mean intensity for subpopulations of the double-labeled FRET sample defined by a successively increasing gate series defined on the intensity scale of sensitized emission („conditional variance" vs. „conditional mean" plots in the *Supplement*).

In the *Experimental results* part, α factors determined in the conventional and the new way are compared: (i) For different labeling ratios of the donor- and acceptor-stained mAbs against the β_2m and heavy chain (h.c.) subunits of the MHCI cell surface receptor. (ii) For two different donor-acceptor dye-pairs (Alexa-Fluor 488-Alexa-Fluor 546 vs. Alexa-Fluor 546-Alexa-Fluor 647, in *Supplement*) to change Förster's R_0 expressing the spectral overlap between the donor and acceptor dyes. (iii) For two different cell lines (FT and LS174T cells) and for treatments of LS174T cells with IFNγ (in *Supplement*) to change the donor intensity levels as well as FRET efficiency via modulation of the surface expression levels of MHCI.

In the *Supplement* we first briefly summarize the conventional FCET method, then a case study is presented as an illustration. An alternative deduction is made of the quadratic equation for α by a unified treatment of the modulations of the donor and acceptor signals during the FRET process. An information theoretical meaning has also been attached to the donor and acceptor moments. Fluorescence lifetime data demonstrating labeling ratio dependence of quantum efficiency and error analysis illustrating stability of α determined as roots of the respective quadratic and cubic equations are presented.

Cells
LS174T colon carcinoma cells (ATCC, Manassas, VA) were kept in continuous logarithmic growth in RPMI 1640 medium supplemented with 10% FCS and 50 µg/ml gentamycin by sub culturing them twice weekly at a concentration of 2.5×10^4 cells/cm^2 with standard trypsinization. For cell activation experiments, cells after sub culturing were treated with 50 ng/ml interferon-γ (IFNγ) (R&D Systems, Minneapolis, MN) and were cultured for an additional 48 h. Kit-225 FT7.10 (FT) cells, a human T-lymphotrophic virus-nonexpressing, cytokine-dependent (IL-2 or IL-15) human adult T lymphoma cell line with a CD4$^+$ phenotype derived from Kit-225 cells [1] were cultured in RPMI medium 1640 supplemented with 10% FBS, penicillin, and streptomycin. We also added 500 pM human recombinant IL-2 to the medium every 48 h. The medium of FT7.10 cells contained 800 µg/ml G418 (GIBCO) to suppress the growth of wild type cells.

Specificity of monoclonal antibodies
The production and specificity of monoclonal antibodies applied in the experimental procedures have been described earlier [2]. Briefly, mAbs W6/32 (IgG$_{2a\kappa}$) and L368 (IgG$_{1\kappa}$) developed against the heavy chain (h.c.) component of the MHCI molecule binding to a monomorphic epitope on the α_2, α_3 domains [3] and the β_2-microglobulin component of MHCI light chain (l.c.), respectively [4], were kindly provided by Dr. Frances Brodsky (UCSF, CA). Fab fragments were prepared from IgGs by papain digestion and were separated from the Fc fragments on protein A-Sepharose column using the method described earlier [5].

Fluorescent staining of mAbs
Aliquots of mAbs and purified Fab fragments were labeled with Alexa-Fluor and indocarbocyanine dyes (Alexa-Fluor 488 as donor, Alexa-Fluor 546 as acceptor or donor, Alexa-Fluor 647 as acceptor, from Invitrogen; Cy5 as acceptor, from Amersham). Kits provided with the dyes were used for the labeling. The detailed staining procedure was described earlier [4-8]. Dye to protein labeling ratios, when asterisk (*) indicates Fab fragments, were: L_d(Alexa-488-L368)=1.1*, 4.9; L_d(Alexa-488-W6/32)=0.85*, 3.4; L_a(Alexa-546-L368)=4.15, 4.7; L_a(Alexa-546-W6/32)=1.5, 2.5; L_a(Alexa-647-L368)=2.1, 5.8; L_a(Alexa-647-W6/32)=1.01*, 1.56, 1.7; L_a(Cy5-L368)=4.2; L_a(Cy5-W6/32)=4.7. The labeling ratios were separately determined for each labeled aliquot in a spectrophotometer (Hitachi U-2900, NanoDrop ND-1000) [2-6]. The labeled proteins retained their affinity as proven by competition experiments with identical, unlabeled ligands.

Labeling of cells with fluorescent ligands
Freshly harvested cells were washed twice in ice cold PBS (pH 7.4). The cell pellet was suspended in 100 µl of PBS (10^6 cells/ml) and labeled by incubation with 10 µg of dye-conjugated ligands (whole mAbs, Fab fragments) for 40 min on ice in the dark [2-6]. The excess of whole mAbs or Fabs was at least 30-fold above the K_d during incubation. To get rid

of possible aggregations of dye-conjugated ligands, they were air-fuged (at 110,000 g, for 30 min) before cell labeling. Labeled cells were washed twice with ice cold PBS and then fixed with 1%-formaldehyde/PBS. Special care was taken to keep the cells at ice cold temperature before FRET measurements in order to avoid unwanted induced aggregations of cell surface receptors or receptor internalization. Data obtained with fixed cells did not differ significantly from those of unfixed, viable cells.

Theory of dual-wavelength flow cytometric resonance energy transfer (FCET)
In the scheme of the FCET method originally published by L. Trón *et al.* in 1984 [9, 10], the energy transfer problem poses the determination of three unknowns on the acceptor and donor labeled cell samples, the donor and acceptor concentrations (represented by signals I_d and I_a bellow) as well as the energy transfer efficiency (E) from three suitable signals (I_1, I_2, I_3) after taking into account the necessary spectral overspills (S_1, S_2, S_3) as „natural characteristics" of FRET-pairs having large enough spectral overlaps. For a summary of the FCET method with the forthcoming extensions, please see also Fig. 1 in the main text. The system of equations contains also a very important 4th parameter, called α, comparing the detectibilities (or „visibilities") of the donor and acceptor signals, whose determination is the central problem in this communication. The I_1 signal (all signals are already background-subtracted), excited at the donors absorption maximum and detected at its emission maximum is the donor fluorescence reduced by possible FRET towards acceptor (quenching) and modified by possible steric interactions between the donor and acceptor targeting labels,

$$I_1 = I_d \cdot (1 - E),\tag{1s}$$

where I_d is the donor fluorescence unperturbed by FRET, but potentially containing the effects of possible steric interactions, and E is the FRET efficiency. Signal I_2, excited at the donor's absorption maximum and detected at the acceptors emission maximum can be decomposed into a first term representing the overspill of the donor emission with the acceptor channel, a second term expressing direct photonic excitation of acceptor at the donor's excitation wavelength, and a third term representing the transferred energy (sensitized emission):

$$I_2 = I_d \cdot (1 - E) \cdot S_1 + I_a \cdot S_2 + I_d \cdot E \cdot \alpha.\tag{2s}$$

The determination of the three unknown parameters requires also a 3rd equation, analogous to Eq. 2s, which is the signal I_3 emitted in the acceptor channel, but excited at the absorption maximum of the acceptor:

$$I_3 = I_d \cdot (1 - E) \cdot S_3 + I_a + I_d \cdot E \cdot \alpha \cdot S_3/S_1.\tag{3s}$$

In Eqs. 2s and 3s, S_1 and S_3 spectral spillage factors determined as

$$S_1 = (I_2/I_1)_{only\ donor},\tag{4s}$$

$$S_3 = (I_3/I_1)_{only\ donor}\tag{5s}$$

on samples labeled only with the donor (also obtainable from Eqs. 2s and 3s by plugging 0 for E, and I_a). Factor S_2, which compares the excitabilities of acceptor at the donor's and

4

acceptor's excitation wavelength (acceptor's bleed through in the donor's excitation channel), can be determined on the sample labeled only with the acceptor according to

$$S_2 = \left(I_2/I_3\right)_{\text{only aceptor}},\tag{6s}$$

as it can be deduced also from Eq. 2s or 3s by plugging zero for E and I_d. With the aid of these parameters, determined by the spectroscopy of the donor and acceptor and the actual optical alignment of the flow cytometer (or microscope), and with the α-factor, detailed later, Eqs. 1s-3s can be solved for E, I_d, and I_a on the double-labeled sample on a cell-by-cell basis in flow cytometry (or in a pixel-by-pixel basis in microscopy) by first introducing a „helper parameter" called A', which plays a crucial role in the elaboration of the present method:

$$A' = E \cdot \alpha/(1-E).\tag{7s}$$

Then expressing I_d from Eq. 1s and inserting into Eqs. 2s, 3s a system of two equations results,

$$I_2 = I_1 \cdot S_1 + I_a \cdot S_2 + I_1 \cdot A',\tag{8s}$$

$$I_3 = I_1 \cdot S_3 + I_a + I_1 \cdot A' \cdot S_3/S_1,\tag{9s}$$

which are conveniently solvable for the unknowns A' and I_a:

$$A' = \frac{I_2 - S_2 \cdot I_3}{(1 - S_2 \cdot S_3/S_1) \cdot I_1} - S_1,\tag{10s}$$

$$I_a = \frac{I_3 - I_2 \cdot S_3/S_1}{1 - S_2 \cdot S_3/S_1}.\tag{11s}$$

Remarkable feature of A' and I_a is that the formulae for their experimental determination (Eqs. 10s, 11s) do not contain α, in spite of the involvement of α in the definition of A' (Eq. 7s). With the aid of A', E is expressed from Eq. 7s as

$$E = A'/(\alpha + A'),\tag{12s}$$

and finally by plugging E into Eq. 1s, I_d is obtained as:

$$I_d = I_1/(1-E).\tag{13s}$$

As it can be seen from Eq. 12s, the α-factor plays a crucial role in the determination of energy transfer efficiency: by comparing Eq. 12s with the „Förster-equation" $E=R_0^6/(R_0^6+R^6)$, A'/α can be identified with $(R_0/R)^6$ – in the original publication of the FCET method A'/α is designated by „A" defined as A=E/(1-E).

A case study on the gating strategy and computation of FRET efficiency in the FCET scheme
The FRET efficiencies, conventional E_0 and correlation-based E, are computed from the background-corrected I_1 (excited at the absorption maximum and detected at the emission maximum of donor, "donor channel"), I_2 (excited at the absorption maximum of the donor and detected at the emission maximum of the acceptor, channel of sensitized emission of acceptor or

"FRET channel"), and I_3 (excited at the absorption maximum and detected at the emission maximum of acceptor, "acceptor channel") intensities of the samples labeled with both donor and acceptor. Computations were done on a cell-by-cell basis by using Eqs. 10s, 12s and for α either Eq. 2 in the main text for the conventional E_0, or Eqs. 9, 20 for the correlation-based E, for the latter also with the assumption that the unperturbed donor moment of the doubly-labeled FRET sample equals that of the donor-only sample i.e. $d=d_0$ (see also Eq. 15 in the main text). Corrections for the spectral overlaps in absorption and emission of the donor and acceptor ("spectral demixing") are made by using the S_1, S_2, and S_3 "spillage factors", which are determined on samples labeled with only the donor (S_1, S_3) or the acceptor (S_2) according to Eqs. 4s-6s. The difference in sensitivities of the donor and FRET channels in detecting a single photon is taken into account with the "scaling factor" α (introduced by Eqs. 2s, 3s) which is determined on the samples labeled with only the donor or the acceptor according to Eq. 2 (conventional way leading to "spectral α" or α_0) and on the double-labeled FRET sample according to Eq. 9 ("correlation-based" leading to α) .

The steps of computation of flow cytometric FRET efficiencies and the necessary gating are illustrated with a case study on the Alexa-Fluor 488-L368 (anti-β_2m)-Alexa-Fluor 546-W6/32 (anti-MHCI h.c.) FRET pair on FT human T-lymphoblast cells. For the computation of a FRET efficiency the following 4 samples are needed with the cell-labeling donor and acceptor mAbs in parentheses:

1. *background* sample (unlabeled with donor or acceptor),
2. *donor* sample (labeled only with Alexa-Fluor 488-L368),
3. *acceptor* sample (labeled only with Alexa-Fluor 546-W6/32), and
4. *FRET* sample (labeled with both Alexa-Fluor-488 L368 and Alexa-Fluor 546-W6/32).

The details of calculations with the used dot-plots and gates are described in Figs. 1s-4s for the common steps of the two approaches. Histograms characteristic to the "correlation-based" approach are shown in Fig. 2 of the main text. All analyses were made with a home-made software ReFlex [11] freely available at http://www.biophys.dote.hu/research.htm or http://www.freewebs.com/cytoflex.htm.

Fig. 1s *Background sample.* The major subpopulation comprising c.a. 80% of the total population of the heterogeneously growing FT cells was separated from the remaining cells and debris based on a gate (red ellipsis) put in the forward light scatter (FSC)-side scatter (SSC) dot-plot. The mean background values as computed from histograms I_1, I_2 and I_3 after activating the above gate – or if necessary from dot-plots I_1-I_2 and I_1-I_3 after putting another two "fine gates" (not shown) in these dot-plots to get reed of outliers – are: $B_1=0.643$, $B_2=0.887$, and $B_3=0.252$. All measured intensities are divided by 1000. These values are subtracted from all fluorescence intensities of the subsequent samples.
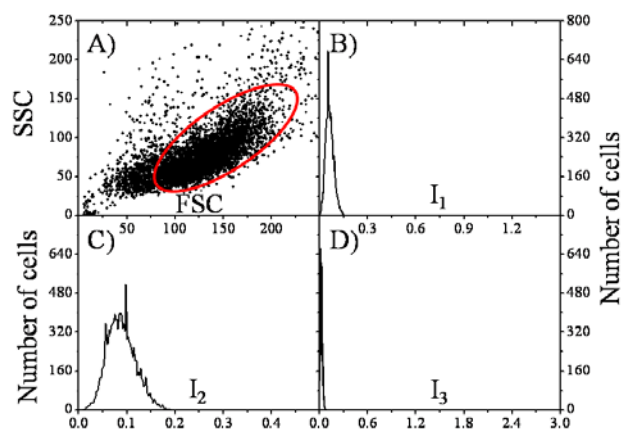
Fig. 2s *Donor sample.* The major subpopulation comprising c.a. 80% of the total population of the heterogeneously growing FT cells was separated from the remaining cells and debris based on a gate (red ellipsis) put in the forward light scatter (FSC)-side scatter (SSC) dot-plot. The I_1-I_2 and I_1-I_3 dot-plots are computed by activating the "initial gate", from which the $S_1 = I_2/I_1$ and $S_3 = I_3/I_1$ histograms are computed – if necessary, after by activating two additional "fine gates" (not shown) put in the I_1-I_2 and I_1-I_3 dot-plots to cut off outlying intensity values. All measured intensities are divided by 1000. Histogram means are: $S_1 = 0.1125$, $S_3 = -0.00014$ which should be plugged into Eq. 10s, 11s above for calculation of I_a (Fig. 4s Panel F) and A', the latter necessary for calculation of both the E_0 and E FRET efficiencies (Eq. 12s) and for the calculation of "correlation-based" α via p and q. Additional parameters required for the calculation of the "conventional" α is $M_d = \overline{I_1}$ (5.989) the

mean of the I_1 distribution and for the "correlation-based" α is d_0 (6.014), the "square of the width" of distribution I_1 (see also Fig. 2 Panel B).
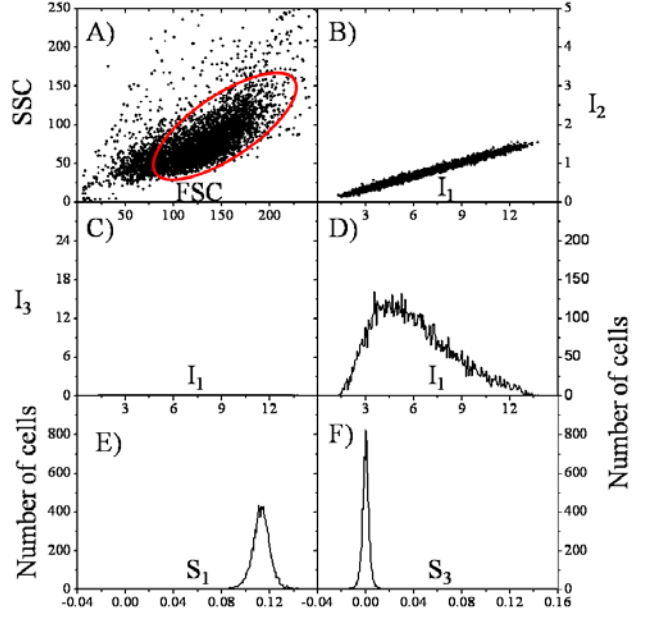
Fig. 3s *Acceptor sample.* The major subpopulation comprising c.a. 80% of the total population of the heterogeneously growing FT cells was separated from the remaining cells and debris based on an "initial gate" (red ellipsis) put in the forward light scatter (FSC)-side scatter (SSC) dot-plot. The I_3-I_2 dot-plot is computed by activating the "initial gate", from which the $S_2 = I_2/I_3$ histogram is computed – if necessary, after by activating a new "fine gate" (not shown) put in the I_3-I_2 dot-plot to cut off outlying intensity values. All measured intensities are divided by 1000. Histogram means are: $S_2 = 0.096$, which should be plugged into Eqs. 10s, 11s above for calculation of I_a (Fig. 4s Panel F) and A', and

$M_a = \overline{I_2}$ (1.2144) the mean of the I_2 distribution
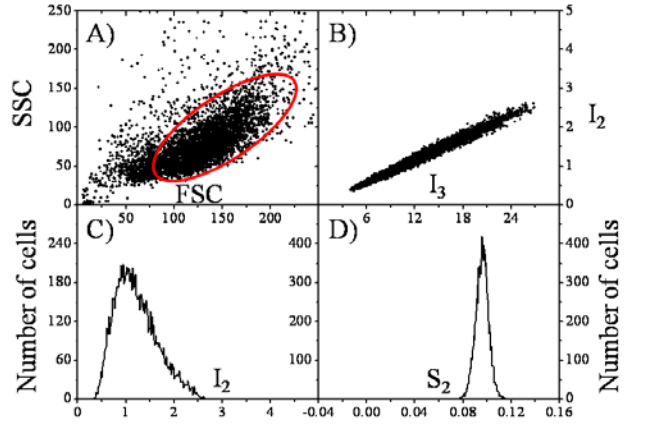
for the calculation of "spectral" α (α_0) according to Eq. 2 in the main text

Fig. 4s *Donor+acceptor together (FRET) sample.* The major subpopulation comprising c.a. 80% of the total population of the heterogeneously growing FT cells was separated from the remaining cells and debris based on an "initial gate" (red ellipsis) put in the forward light scatter (FSC)-side scatter (SSC) dot-plot. The I_1-I_2, I_1-I_3 and I_3-I_2 dot-plots are computed by activating the "initial gate", and all the subsequent histograms (A', d', p, q, α, Q, E) are computed from these latter dot-plots – if necessary, after by activating a new "fine gates" (not shown) put in the I_1-I_2, I_1-I_3 and I_3-I_2 dot-plots to cut off outlying intensity values. All measured intensities are divided by 1000. The "spectral α" (α_0) calculated in the conventional way as $\alpha_0 = (\varepsilon_d/\varepsilon_a)\cdot(L_d/L_a)\cdot(B_d/\mathbf{B}_a)\cdot(M_a/M_d) = 4.16$ with $L_d=5.0$, $L_a=1.5$ labeling ratios of the donor and acceptor antibodies; the B_d/B_a ratio of the labeled binding sites (in this case unity, being the labeled epitopes two subunits of the same MHCI

molecule); the ratio of the absorption coefficients of the donor and acceptor at the wavelength of excitation of the donor $\varepsilon_d/\varepsilon_a=6.21$ ($\varepsilon_d= 75.2\%$ of $\varepsilon_{max}=73000$ M^{-1}cm^{-1} for Alexa-Fluor-488, $\varepsilon_a= 7.89\%$ of $\varepsilon_{max}=112000$ M^{-1}cm^{-1} for Alexa-Fluor-546 at 488 nm-excitation); and the ratio $M_a/M_d=0.202$, where $M_d=5.989$ is the mean donor intensity in the signal channel I_1 for the sample labeled with only donor (Fig. 2s, Panel D) and $M_a=1.2144$ is the mean acceptor intensity in the signal channel I_2 for the sample labeled with only acceptor (Fig. 3s, Panel C), after subtracting the corresponding background intensities (Fig. 1s). The "correlation-based α" (0.1) is calculated by using Eqs. 9-12 of the main text, with input parameters d $\approx d_0$ (6.014) determined from the donor-only sample, and d' (1.0445),p (0.1147), q (0.0194) all determined from the double-labeled sample (for distribution of these quantities, see Fig. 2 Panels B-E). The FRET efficiency as calculated with the "correlation-based" α is E=46.9%, the donor quenching is Q=44.5%, and A'=0.091 (for distributions see Fig. 2 Panels F-H). In the knowledge of distribution of E, the distribution of the unquenched donor intensity of the double-labeled sample I_d (mean value: 3.3258) is calculated according to Eq. 13s (Fig. 4s, Panel E).
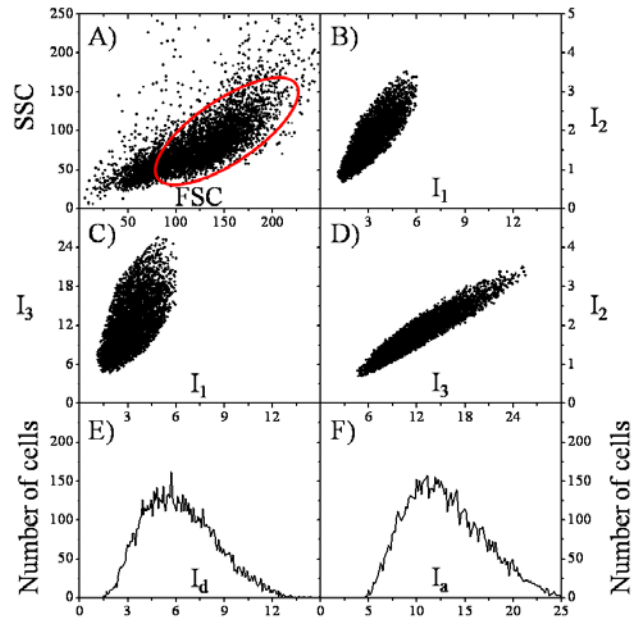
Comparative measurements of FRET between epitopes of MHCI at different labeling ratios of mAbs on the surface of FT T-lymphoblast cells: (II.) Alexa-Fluor 488-Alexa-Fluor 546 dye pair

The intra-molecular FRET measurements in the L368 →W6/32 direction pertinent to data of Table 1 in the main text, and both intermolecular FRET measurements (L368-L368, W6/32-W6/32) were repeated on the same cell line with the Alexa-Fluor 488-Alexa-Fluor 546 dye-pair (Table 1s). By inspecting data in Table 1s Part A we can see that the „covariance-based" α-factors are considerably smaller than the conventional α-factors (α_0), leading to E values much larger than E_0, due to the large labeling ratio at the donor side ($L_d=5$). When compared to the quenching efficiency Q, one accepts E as the true transfer efficiency, being Q equal to E, rather than to E_0, the same result as obtained above with the Alexa-Fluor 546-Alexa-Fluor 647 dye-pair (Table 1 in main text). We remark here also that, although the α-factor depends on the „momentary" optical condition of the cytometer (i.e. on the daily optical alignment), its much smaller value for the Alexa-Fluor 488-Alexa-Fluor 546 dye-pair than for the Alexa-Fluor 546-Alexa-Fluor 647 dye-pair informs us about a much larger difference in sensitivity between the green and red signal channels (α is smaller) than between the two red signal channels (α is larger), as expected.

By inspecting the FRET data pertinent to measurement of homo-associations with the L368 and W6/32 mAbs (Table 1s, Part B), in contrast the much larger α factors obtained with the conventional method (α_0), after correcting the coefficient of the leading quadratic term in Eq. 9 according to Eq. 19 (in main text), essentially the same values were obtained for α_{cubic} as for α_0, implying equal values for E_0 and E.

Table 1s. Conventional and the covariance-based alpha-factors as well as the deduced FRET-efficiencies measured between the β_2m (l.c.) and heavy chain (h.c.) subunits of the MHCI receptor as well as between its heavy chain subunits on the surface of FT T-lymphoblast cells by using Alexa-Fluor 488- and Alexa-Fluor 546-conjugated mAbs

FRET-pairs				Labeling ratio		Alpha-factors			FRET efficiencies (%)		
Donor: Alexa-Fluor 488		Acceptor: Alexa-Fluor 546				Spectral	Covariance-based		Quenching	Quenching & sensitized emission	
mAb	Epitope	mAb	Epitope	L_d	L_a	α_0 [a)]	α [b)]	α_{cubic} [c)]	Q [d)]	E_0 [e)]	E [f)]
Part A											
L368		W6/32				4.16	0.10	-	44	2	39
L368	β_2m	W6/32 low [g)]	MHCI h.c.	5.0	1.5	4.05	0.12	-	35	2	30
L368 low [g)]		W6/32				4.16	0.14	-	45	2	38
Part B											
L368	β_2m	L368	β_2m	5.0	4.7	0.16	0.06	0.16	57	25	25 [h)]
W6/32	MHCI h.c.	W6/32	MHCI h.c.	3.4	1.5	0.57	0.06	0.15	64	8	25 [h)]

[a-i)] With the same meaning of these marks as for Table 1 in main text.
[h)] These values were calculated by using α_{cubic}, the solution of Eq. 20 with m=1.31, b=0.13 (R^2=0.93) obtained by fitting the corresponding Q-Q' plot like that shown in Fig. 3 Panel A.

Comparative measurements of FRET between epitopes of MHCI at different labeling ratios of mAbs on the surface of LS174T-cells

To see the consistency of the „covariance-based" FRET determination at different signal levels – mainly governed by the expression level and degree of homo-association of MHCI in addition to the labeling ratios of the applied mAbs implying altered donor-acceptor ratios and FRET efficiencies – the above experiments on the MHCI proximities were repeated on a different cell line, LS174T colon carcinoma cells. In addition to that the MHCI level on this cell line is c.a. 30% of that on FT cells (29.8±8.9%) the degree of homo-association of MHCI is also considerably smaller. The signal levels also have been modulated by treatments of these cells with the cytokine IFNγ. Interestingly, while IFNγ doubled the expression level of MHCI (190±10%), the degree of its homo-association was reduced, supposedly due to the intercalation of the „intercellular adhesion molecule-1" (ICAM-1) not measured in this study [7]. FRET data on the Alexa-Fluor 546-Alexa-Fluor 647 and on the Alexa-Fluor 546-Cy5 dye-pair are listed in Table 2s. By inspecting Parts A and C it can be seen that the due to the small labeling ratios, the conventional and „covariance-based" α-factors are close to each other, implying a similar relationship between the deduced E_0 and E FRET efficiencies. Moreover in the L368 Fab→W632 intramolecular FRET case, these FRET efficiencies are also close to the quenching efficiency Q, in contrast to the intermolecular cases L368 Fab→

L368 Fab and W6/32→W6/32 when E_0 and E both are much smaller than Q, due to the competition between the dye-targeting mAbs.

When inspecting Part B of Table 2s, the usual behavior can be seen again: Due to the high labeling ratio of the donor-targeting mAb, the conventional „spectral" α-factor is an upper-estimation of the true α, leading to corresponding under-estimation of the true FRET efficiency. However, the covariance-based α-factor gives an acceptable deduced FRET efficiency E also in this case, as proven by its good correspondence with the Q quenching efficiency (Q depending on both competition and FRET, while E_0 and E depending only on FRET).

As to the Alexa-Fluor 546-Cy5 FRET system, by examining Table 2s Part D an interesting observation is that in spite of the large value of the labeling ratio of the acceptor-targeting mAb, the conventional and the „covariance-based" α-factors are practically the same, leading to the same deduced FRET efficiencies. This result implies that at large local concentrations the Cy5 dye behaves differently from the Alexa-Fluor dyes, and/or the dye-conjugation sites for this dye on the W6/32 mAb is such that it does not impairs mAb binding to its epitope on the h.c. subunit of the MHCI receptor.

Table 2s. Conventional and the covariance-based alpha-factors as well as the deduced FRET-efficiencies measured between the β_2m and heavy chain (h.c.) subunits of the MHCI receptor as well as between its heavy chain subunits on the surface of LS174T colorectal carcinoma cells by using Alexa-Fluor 546- and Alexa-Fluor 647- or Cy5-conjugated mAbs.

FRET-pairs				Treat-ment [a]	Labeling ratio		Alpha-factors			FRET efficiencies (%)		
							Spectral		Covariance-based	Quenching		Quenching & sensitized emission
Donor		Acceptor										
mAb	Epitope	mAb	Epitope		L_d	L_a	α_0 [b]	α [c]	α_{cubic} [d]	Q [e]	E_0 [f]	E [g]
Part A: Alexa-Fluor 546-Alexa-Fluor 647												
L368 Fab	β_2m	W6/32	MHCI h.c.	Cont.	0.8	1.6	0.16	0.15	-	17	18	20
				IFNγ			0.16	0.15	-	17	20	21
Part B: Alexa-Fluor 546-Alexa-Fluor 647												
L368	β_2m	W6/32	MHCI h.c.	Cont.	6.5	2.2	2.42	0.48	-	27	9	34
				IFNγ			2.49	0.55	-	26	8	28
Part C: Alexa-Fluor 546-Alexa-Fluor 647												
L368 Fab	β_2m	L368	β_2m	Cont.	0.8	2.1	0.16	0.05	0.25	63	25	16 [h]
				IFNγ			0.10	0.03	0.14	57	14	11 [h]
Part D: Alexa-Fluor 546-Cy5												
L368 Fab	β_2m	W6/32	MHCI h.c.	Cont.	0.8	4.7	0.16	0.17	-	36	41	40
				IFNγ			0.16	0.19	-	29	39	29

[a] Cells have been treated with IFNγ and at 50 ng/ml concentration, for two days before harvesting.

[b] The conventional (or spectral) alpha-factors (α_0) have been calculated according to Eq. 2 of the main text by using the mean intensities of the samples labeled only with the donor and the acceptor as well as the labeling ratios and absorption coefficients. Due to the 1:1 stoichiometry of the two subunits of the same MHCI molecule, unity was used for the ratio of the labeled receptors (B_d/B_a). All data in this table are representative ones of three different measurements giving similar results, with relative errors <15% (SEM/mean).

[c] Covariance based alpha-factor at the donor side (α) was determined as the mean value of the corresponding cell-by-cell distribution of α obtained as the positive root of the quadratic polynomial in Eq. 9 written for the cell-by-cell distributions of the D, p and q coefficients, examples of which are shown in Fig. 2. In the calculation of the D coefficient in Eq. 9, for the non-competing case of FRET measurement between the β_2m and h.c. subunits, the d value of the FRET sample was approximated by the mean of d_0 distribution of the corresponding single-donor labeled sample.

[d] In the case of FRET indicating homo-association between the MHCI receptors, instead of using d_0 of the single-donor labeled sample, the d value has been approximated from the d' value of the FRET-sample according to Eq. 19 and the positive root of the cubic polynomial in Eq. 20 resulting in a meaningful FRET efficiency (α_{cubic}) was used in the calculation of E. We remark that while the root of the quadratic polynomial of Eq. 9 has been found for each cell and the cell-by-cell distribution of α has been determined, this latter calculation have been carried out only with mean values.

[e] Quenching efficiency (Q) is defined as the relative change in the I_1 donor fluorescence due to the mAb used as acceptor. Mean values of the corresponding cell-by-cell distributions, defined as $Q=1-I_1/I_{1,d}$ where I_1 is intensity of the double-labeled sample and $I_{1,d}$ is the mean intensity of the sample labeled only with the donor, are listed. In the case of competing mAbs for the measurement of MHCI homo-association, it contains also the intensity reducing effect of mAb competition in addition to the effect of FRET.

f) E_0 has been calculated as the mean of the corresponding cell-by-cell distribution obtained from the A' distribution by using $E_0=A'/(\alpha_0+A')$ (Eq. 12s) with the conventional alpha-factor (α_0) as an input constant.

g) E has been calculated as the mean of the corresponding cell-by-cell distribution obtained from the A' distribution by using $E=A'/(\alpha+A')$ with the covariance-based alpha-factor (α) as an input constant. These values were calculated by using α_{cubic}, the solution of Eq. 20 with m=3.2, b=0.13 ($R^2=0.75$) obtained by fitting the corresponding Q-Q' plot like that shown in Fig. 3 Panel A.

Fluorescence lifetime measurement by FLIM

Fluorescence lifetimes of the Alexa-Fluor 488 and Alexa-Fluor 546 dyes conjugated to the L368 and W6/32 mAbs at different labeling ratios have been measured on the cell surface with the FLIM technique. The cell types and processing of the cells have been the same as for flow cytometry. The basic FLIM arrangement – a homodyne detection scheme of phase and modulation lifetimes – has been built around a wide field fluorescence microscope (E-600, Nikon, objective Plan Apo 60x, NA=1.2, water immersion). For the principles and detailed technical description of the homodyne lifetime detection such as camera, image intensifier, signal generators, and signal amplifier we refer to [12]. Briefly: A light emitting diode (LED) (Luxeon III Star, LXHC-LB3C, Lumileds Lighting, US, CA) has been used for illumination (470 nm, 30 mW), the power supply of which was modulated at the same frequency (60 MHz) but at different phases relative to the modulation of the image intensifier. The fluorescence signal channel, corresponding to the I_1 signal of the FCET method, was specified by a 470±15-nm excitation filter (HQ470/30, AF Analysentechnik, Tübingen); a 505DRLP02 dichroic mirror and a 525±15-nm emission filter (525DF30, Omega Optical, Brattleboro, VT). For calibration a standard solution of fluorescein having a 4 nsec-lifetime was used.

Fluorescence lifetime depends on the labeling ratios of mAbs

Seeking for possible reasons for the differences between the conventional (or „spectral") α_0 and the α-factor obtained with the correlation method observed at large dye-per-antibody labeling ratios we measured fluorescence lifetime (proportional with quantum yield) as the function of labeling ratio with the FLIM technique. By applying the phase-modulation method we observed monotonous decreases of phase-lifetime with increasing labeling ratios for the Alexa-Fluor 488-conjugated L368 mAb (a 34.1%-reduction: τ_{phase}=3.93±0.05, 3.25±0.13, 2.59±0.03 ns at labeling ratios L_d=1.5, 1.6, 2.1) and for the Alexa-Fluor 488-conjugated W6/32 mAb (a 28.1%-reduction: τ_{phase}=3.56±0.09, 3.32±0.10, 3.08±0.12, 2.56±0.03 ns at labeling ratios L_d=0.9, 1.0, 2.7, 3.6), n>5 in both cases (Fig. 5s, Panels A, B). The trends can be well fitted with straight lines having slope (s) and intersection (i) s=-1.8, i=6.4 for L368 ($R^2=82.5\%$), and s=-0.3, i=3.8 for W6/32 ($R^2=90.3\%$). In the case of W6/32, with the same labeling ratios the modulation lifetime shows also a similarly decreasing tendency, albeit with a smaller rate than for the phase-lifetime (a 14.1%-reduction: τ_{mod}=3.54±0.04, 3.14±0.06, 3.24±0.05, 3.04±0.03). As a result, the ratio of modulation and phase-lifetimes, a measure of lifetime heterogeneity [12, 13], slightly increases with the labeling ratio (a 20%-increase: τ_{mod}/τ_{phase} =0.99, 0.95, 1.05, 1.19) in accordance with the view that the number of non-emitting, dark complexes and consequently, the rate of FRET towards these complexes may

increase. Similar decreases in lifetime but with much larger magnitudes were observed for the Alexa-Fluor 546-conjugated L368 mAb (a 59.7%-decrease for the phase-lifetime: τ_{phase}=2.01±0.03, 1.45±0.04, 0.81±0.09, and a 53.3%-decrease for the modulation-lifetime: τ_{mod}=3.19±0.01, 2.48±0.01, 1.49±0.03 at L_a=1.2, 2.7, 3.5), and only a modest (15%) increase in the lifetime ratio similarly to the Alexa-Fluor 488 (Fig. 5s, Panel C). However, when the absolute values of lifetime ratios are compared, these are much larger for Alexa-Fluor 546 than for Alexa-Fluor 488 (1.6 vs. 1.0 at the smallest labeling ratios, Fig. 5 Panels B, C), implying a much larger tendency for complex formation for Alexa-Fluor 546.

Fig. 5s *Fluorescence lifetimes of dye-conjugated mAbs as the function of labeling ratio.* Phase and modulation lifetimes (τ_{phase}, τ_{mod}) and their ratio (τ_{mod}/τ_{phase}) as measured with the FLIM technique. While the phase and modulation lifetimes monotonously decrease, their ratio increases with increasing labeling ratio of the dye-targeting mAbs, implying increasing interaction between the dyes with the increasing local concentration. The interaction is largely mediated by homo-FRET being the critical Förster-distance comparable to the size of mAbs: $R_{0, \text{Förster}}$~4 nm vs. ~3.5 nm smaller and ~6.5 nm larger diameter of an Fab-fragment as a rotational ellipsoid [14]. The increasing lifetime ratio indicates increasing lifetime heterogeneity in accordance with the increased number of different dye microenvironments. Panel A: Alexa-Fluor 488-conjugated L368, Panel B: Alexa-Fluor 488-conjugated W6/32, Panel C: Alexa-Fluor 546-conjugated W6/32. Error bounds are within the size of symbols.
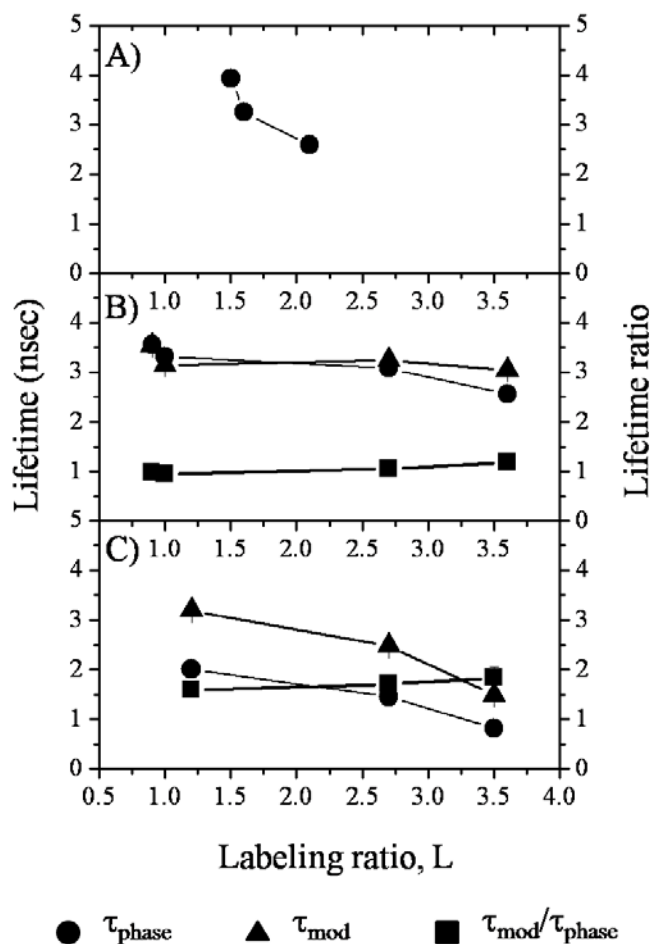
Overview of the correlation method
The point in the newly developed method is that besides the conventional system of equations (Eqs. 1s-3s in *Supplement*) characterizing the FRET-system, based on „suitably defined" variance and covariance terms calculated from intensities of the donor-only and FRET samples (labeled with only donor, and with both donor and acceptor, respectively), a quadratic equation (Eq. 9) can be set up for the α factor whose positive root serves as the accepted value of α (see Fig. 1 for a summary of the new method). Advantageous properties of the quadratic equation are that: (i) The positive root is always existing. (ii) Because the covariance and variance are averages of the corresponding fluctuation products and squares, an analogue quadratic equation can be formulated also for the corresponding fluctuation square and product terms, which by the fact that they can be determined on a cell-by-cell

basis, enables the determination of α factor for each individual cell, i.e. it enables the determination of the cell-by-cell distribution of α factor (Fig. 2, Panel E). (iii) Although essentially two samples are needed for the determination of the α factor (notwithstanding now the determination of the spillage factors), the donor-only (for d_0) and the FRET samples (for d'), it can be shown that this rigor can be significantly relaxed if the variation of donor-moment is known as the function of the donor intensity (Q'-Q plots, Fig. 3 Panel A), when the α factor is determined on the very double-labeled sample from which the FRET efficiency is eventually calculated (by Eq. 20). (iv) By approximating d with d_0 gives the true value for α in the absence of any competition of the dye-targeting ligands (or other non-FRET interaction), α is underestimated, and consequently E is upper-estimated in the presence of it.

Comparative measurements of FRET at different labeling ratios of mAbs reveal differences in the conventional and covariance-based FRET determinations
In the framework of the FCET-method, as it has been originally worked out by Trón *et al.* [9, 10] the α-factor is determined based on the mean intensities of the donor- and acceptor-only samples in the knowledge the relative absorption coefficient of the donor and the acceptor ($\varepsilon_d/\varepsilon_a$) at the excitation wavelength of the donor, the labeling ratios of the donor- and acceptor-conjugated ligands (L_d, L_a), and the numbers of the labeled receptors (B_d, B_a) (Eq. 2). According to the correlation-based method, the α-factor is determined by the positive root of Eq. 9 which is simple quadratic in those cases when the coefficient of the quadratic term (D) can be calculated with the intensity moment of the donor-only sample (d_0) as an input parameter (D=d_0-d'), i.e. as far as there is no steric interaction between the labels.

When comparing the α-factors determined in the two ways obtained in measurements of FRET between the epitopes of MHCI (Tables 1, 2, 1s), we can recognize that one important factor behind their possible deviation is the labeling ratio (L_d, L_a) of the used dye-conjugated ligands. While for small labeling ratios around unity (in the range 0.5-2), good correspondence can be found between the two kinds of α, at large ones (>3) substantial deviations may occur, but not necessarily, possibly depending on the position of dye-conjugation sites on the ligands. Alternatively two errors, one in the numerator and another in the denominator, committed in the determination of the labeling ratios (L_d, L_a) and/or binding sites (B_d, B_a) could cancel each other in Eq. 15. Based on published data of others [15-20], as well as our own experience there are two main factors governing brightness (effective fluorescence) of dye-conjugated ligands: (i) spectral interactions of the spatially confined dyes, facilitated by the large local concentrations due to the small ligand size – e.g. 1 dye in an area of an effective diameter of an Fab fragment (5 nm) means 85 mM local concentration, and (ii) impaired binding of ligand to its receptor due to shielding of binding sites by the dressing dyes.

(i) As to the spectral interactions, the large local concentrations can favor the formation of dark complexes with their absorption spectra shifted towards larger wavelengths, favoring hetero-FRET from monomers towards complexes, which is accelerated by possible homo-FRET between the monomers in close proximity (FRET cascade), being the characteristic Förster distance ~ 4nm, comparable to the radius of an mAb ~6.5 nm [14]. This result in acting of dark complexes as traps for the excitation energy [20], manifested in a decrease in quantum yield, or equivalently in the „effective dye-per-protein labeling ratio". This physical picture is corroborated by the fact that fluorescence anisotropy of these mAbs decrease with increasing labeling ratio [21]. Alternatively, this same phenomenon can also be treated in terms of reduced lifetime, being lifetime proportional to the quantum yield, as observed by us with fluorescence lifetime imaging microscopy (FLIM) (Fig. 5s). Physically this implies that, the error is committed by not using the effective absorption coefficients

corresponding to the number of FRET events. While on the donor side the absorption is over-estimated, on the acceptor side under-estimated.

Mathematically the reason of the error is in assuming linear relationship between fluorescence and the labeling ratio in Eq. 2 [15]. Although in some cases (e.g. mAbs) there is a possibility to correct mathematically this error by using the appropriate functional dependence after suitable calibration of the ligand fluorescence (measurements of quantum yields and lifetimes as the function of labeling ratio on the cell surface) we favor our method using the in-situ intensity correlations on the cell surface, because quantum yield calibration is generally not easily done and lifetime measurements are not readily available on the surface of living cells.

(ii) The other possible candidate behind the error could be the effect of shielding of binding sites (directed towards the receptors) on the ligands by the conjugated dyes, leading to the reduction in the effective labeling ratio of the ligands actually bound to the receptors as compared to the unbound ligands – a kind of „sieving property" in terms of the number of the effectively bound dyes. That this „sieving property" may operate at large dye-per-protein labeling ratios is indicated by our experience that the intensity reduction of the bound ligands maybe larger than the reduction in effective lifetime.

Fig. 6s *Dependence of FRET indices on the labeling ratios of mAbs.* While the trends of all FRET-indices are similar at small donor labeling ratios (<4) and small L_d/L_a values (<1.4), the trend of E_0 (Panels G, H, I) deviates from those of E, Q, and Q' towards small values at large donor labeling ratios (>4) and large L_d/L_a values (>1.4), in accordance with the observed bad correlations of E_0 with E, Q and Q' (Fig. 3 Panels B, C, E in the main text). While all FRET indices with the exception of E_0 stay constant with the donor labeling ratio L_d (1st column), they all increase with the acceptor labeling ratio L_a (2nd column). This observation seems to be corroborated by that increasing L_d/L_a reduces FRET (3rd column).
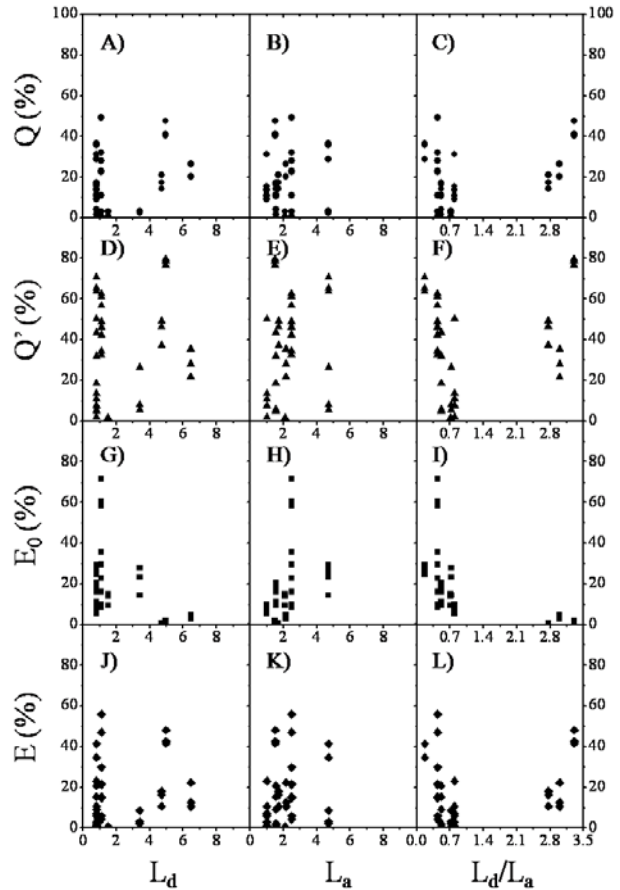
Estimating intensity variation of d from a single cell-by-cell distribution of the I_1 donor intensity

For determining the functional form of the dependence of Q' on Q, measurements of I_1 on at least 2-3 different donor samples are needed. However there could occur practical cases (e.g. rare genetically engineered protein samples) when only a single donor sample is available. For handling these cases the question arises whether the intensity variation of the second moment of the intensity distribution (i.e. the dependence of the distribution width on the mean intensity) can be forecasted by using the intensity distribution of a single sample either singly donor labeled, or doubly labeled with both donor and acceptor.

According to our experience, an approximation can be obtained by successive gating on the I_2 intensity axes of the I_1-I_2 correlation dot-plots. In this procedure the $I_{2,min}$- $I_{2,max}$ range of the I_2 intensity is divided into a number of intervals (n=20 is adequate in practice), such a way that each interval has the same $I_{2,min}$ as left endpoint, and the right endpoint is successively increases with the same width of w= $(I_{2,max}$- $I_{2,min})$/n. This way a series of increasing intervals is obtained such a way that each interval contains the previous one as a subset and the last interval coincides with the total $I_{2,min}$-$I_{2,max}$ interval itself. The interval series defined on the I_2 axis fixes a corresponding series of distribution on the I_1 axis, with the largest one the distribution I_2 itself („conditional distributions", where instead of I_2 could also be I_3, FSC, SSC). By plotting the individual moments („conditional variances") [22] of the members of this series as the function of the respective mean values („conditional means") a curve is obtained which is characteristic to the intensity distribution. By fitting this curve with an appropriate function („trend line") an analytic form can be obtained which can be used for estimating the unknown d value from the measured d' and A'. According to our experience the best fit having a correlation coefficient close to unity is an exponential of the form

$$d = p_{1,fit} \cdot e^{p_{2,fit} \cdot I_d}, \tag{14s}$$

with limiting values $d(I_d = \overline{I_1})$=d_0 on the donor-only sample, and $d(I_d = \overline{I_1})$=d' on the double-labeled sample (where $\overline{I_1}$ now designates the right end-point of the I_d values, which is the mean of the I_1 distribution). Because FRET generally means only a modest perturbation of the I_1 intensity distribution, the „work function" in Eq. 14s can equally well be applied for both the singly labeled and doubly labeled samples with approximately the same fitting constants. For the sake of comparison with the previous procedure of fitting the Q'-Q curves, a linearized version of the exponential in Eq. 14s can be obtained by giving the equation of the tangent line at the right end-point (i.e. at $\overline{I_1}$):

$$d = m' \cdot I_d + b', \tag{15s}$$

with

$$m' = p_{1,fit} \cdot p_{2,fit} \cdot e^{p_{2,fit} \cdot \overline{I_1}}, \tag{16s}$$

$$b' = p_{1,fit} \cdot e^{p_{2,fit} \cdot \overline{I_1}} - m' \cdot \overline{I_1}. \tag{17s}$$

That the two procedures (fitting of the Q' vs. Q curve in Eq. 18 and the fitting of the exponential in Eq. 14s) lead to the same results is also proved by the fact that the coefficients of the trend line in Eq. 18 are almost the same as those in Eq. 14s. After fixing the coefficients of the trend line in Eq. 14s and expressing I_d based on Eq. 5 as the function of A' and α, d can

be expressed as the function of A' and α and plugged into Eq. 9 via Eq. 10, thereby arriving at the following transcendental equation for α:

$$\left[p_{1,\text{fit}} \cdot e^{p_{2,\text{fit}} \cdot \overline{I_1} \cdot \left(1 + \overline{A'}/\alpha\right)} - d'\right] \cdot \alpha^2 - 2 \cdot p \cdot \alpha - q = 0, \tag{18s}$$

where the upper bars designate averaging. The „relevant" roots (positive and „large enough" for producing E<1) of Eq. 18s serve as α. When d is expressed with A' and α via the approximating tangent line of Eq. 14s, Eq. 18s will reduce to a cubic polynomial, like in the case of Eq. 18 as already discussed above.

As to the experimental results, in the case of the Alexa-Fluor 546-L368-Alexa-Fluor 647-W6/32 FRET-pairs of Table 1 Panel A: α=0.38, 0.24, 0.50 for each entry, respectively, with fitting parameters $p_{1,\text{fit}}$=0.059, $p_{2,\text{fit}}$=2.215 (R^2=0.98), for the L368-L368 and W6/32-W6/32 FRET-pairs of Table 1 Panel C: α=0.18, 0.20, respectively, with fitting parameters $p_{1,\text{fit}}$=0.059, $p_{2,\text{fit}}$=2.215 (R^2=0.95), and $p_{1,\text{fit}}$=0.21, $p_{2,\text{fit}}$=0.255 (R^2=0.96). In the case of the Alexa-Fluor 488-L368-Alexa-Fluor 546-W6/32 FRET-pairs of Table 2 Panel A: α=0.09, 0.10, 0.15 with the fitting parameters $p_{1,\text{fit}}$=0.023, $p_{2,\text{fit}}$=0.930 (R^2=0.99).

Estimating d by using Eq. 2, a hybrid approach, when the labeling ratios are small
In this case we assume that Eq. 2 for the α is strictly valid (as is the case for labeling ratios around unity), and that the donor-to-acceptor concentration ratio (B_d/B_a) is the same and known value for each individual cell (or pixel). By isolating the ρ "absorbance ratio" in Eq. 2 as

$$\rho = \frac{\varepsilon_d \cdot L_d \cdot B_d}{\varepsilon_a \cdot L_a \cdot B_a}, \tag{19s}$$

and replacing M_a and M_d with $S_2 \cdot I_a$ and I_d of the double-labeled sample, respectively, we arrive at an alternative form of Eq. 2, which is applicable on a cell-by-cell basis:

$$\alpha = \rho \cdot S_2 \cdot I_a / I_d . \tag{20s}$$

The use of Eq. 20s is in that it connects the unknown unperturbed donor moment (d) introduced in Eq. 7 to the acceptor moment

$$d_a = \left(I_a, I_a\right), \tag{21s}$$

which is measurable also on the FRET sample (for I_a see Eq. 11s):

$$d = \left(\rho \cdot S_2 / \alpha\right)^2 \cdot d_a . \tag{22s}$$

This form of d – via also Eq. 10 for D – results in an alternative form of Eq. 9 defining α:

$$d' \cdot \alpha^2 + 2 \cdot p \cdot \alpha + \left[q - \left(\rho \cdot S_2\right)^2 \cdot d_a\right] = 0 , \tag{23s}$$

which can be used for determining α on a cell-by-cell basis as far as ρ is a known constant value for each cell – e.g. in the case of two subunits of the same MHCI receptor, or when homo-association is measured. Expanded form of the constant term of Eq. 23s as the function of the moments of I_1, I_2 and I_3 can be obtained from the expanded form of q (Eq. 14) by the following replacements of (I_2, I_2), (I_2, I_3), and (I_3, I_3) via Eq. 11s for I_a:

$$\left(I_2, I_2\right) \rightarrow \left[1 - \left(\rho \cdot S_2 \cdot S_3 / S_1\right)^2\right] \cdot \left(I_2, I_2\right), \tag{24s}$$

$$(I_2, I_3) \rightarrow \left[1 - \rho^2 \cdot S_2 \cdot S_3 / S_1 \right] \cdot (I_2, I_3), \tag{25s}$$

$$(I_3, I_3) \rightarrow (1 - \rho^2) \cdot (I_2, I_3). \tag{26s}$$

Acceptor moments: alternative deduction of Eq. 9 for α and entropic interpretation of the moments

Further insight into the physical meaning of the coefficients D, p, and q for the quadratic polynom defining α (Eq. 9) can be gained by taking into account also the moments of acceptor and by taking the sum of the donor and acceptor signals as a whole. The idea is that although FRET reduces donor signal and enhances acceptor signal separately in the donor and acceptor channels, and consequently changes the corresponding individual moments similarly, it does not affect the sum of the donor and acceptor signals and the moment of the sum. If the donor energy is designated by ξ, acceptor energy by ψ, and the transferred energy by ζ, then $(\xi + \psi)_{no\,FRET} = [(\xi - \zeta) + (\psi + \zeta)]_{with\,FRET}$, so the moments of the total signal before and after FRET should be the same. By going over to the language of moments and applying Eqs. 1s, 2s of the *Supplement*:

$$(\alpha \cdot I_d + I_a \cdot S_2, \alpha \cdot I_d + I_a \cdot S_2)_{no\,FRET} = \tag{27s}$$
$$= (\alpha \cdot I_d \cdot (1 - E) + I_a \cdot S_2 + \alpha \cdot I_d \cdot E, \alpha \cdot I_d \cdot (1 - E) + I_a \cdot S_2 + \alpha \cdot I_d \cdot E)_{with\,FRET}.$$

By replacing $I_d \cdot (1 - E)$ with I_1 (Eq. 1s), and by replacing $\alpha \cdot I_d \cdot E$ with $I_1 \cdot A'$ (deducible from Eqs. 12s, 13s):

$$(\alpha \cdot I_d + I_a \cdot S_2, \alpha \cdot I_d + I_a \cdot S_2)_{no\,FRET} = \tag{28s}$$
$$= (\alpha \cdot I_1 + I_a \cdot S_2 + I_1 \cdot A', \alpha \cdot I_1 + I_a \cdot S_2 + I_1 \cdot A')_{with\,FRET}.$$

Although the acceptor channel I_2 contains as a portion the overspill of the donor into this channel, we left out from the expression of the total signal, to contain only the real contributions of the donor and the acceptor. If now the acceptor moment without FRET and with FRET is designated by d_a' and d_a'' and defined with I_a (Eq. 11s) and A' as follows:

$$d_a' = (S_2 \cdot I_a, S_2 \cdot I_a), \tag{29s}$$

$$d_a'' = (I_a \cdot S_2 + I_1 \cdot A', I_a \cdot S_2 + I_1 \cdot A'), \tag{30s}$$

Then from Eq. 28s the difference of donor moments without and with FRET (which is the leading term of Eq. 9) can be expressed in terms of the acceptor moments:

$$(d - d') \cdot \alpha^2 = d_a'' - d_a' + 2 \cdot [\alpha \cdot (I_1, I_1 \cdot A') - S_2 \cdot (I_a, I_1 \cdot A')]. \tag{31s}$$

After expending d_a'' in Eq. 30s, the d_a''-d_a' difference in Eq. 31s can be replaced by

$$d_a'' - d_a' = 2 \cdot S_2 \cdot (I_a, I_1 \cdot A') + (I_1 \cdot A', I_1 \cdot A'), \tag{32s}$$

arriving at

$$(d - d') \cdot \alpha^2 = 2 \cdot (I_1, I_1 \cdot A') \cdot \alpha + (I_1 \cdot A', I_1 \cdot A'), \tag{33s}$$

which is just Eq. 9, the quadratic equation already deduced for α determination, with $D = d - d'$, $p = (I_1, I_1 \cdot A')$, $q = (I_1 \cdot A', I_1 \cdot A')$. The significance of this formalism is not only in that it enabled a second way of deduction of Eq. 9, but also that it enables us to attach physical interpretations to the meaning of the donor and acceptor moment differences and covariances. (i) Based on Eq. 33s the reduction in donor moment has two sources: the first term is the modulation of the remaining donor signal (I_1) by the transferred energy ($I_1 \cdot A'$), and the second term is the moment of the transferred energy. The interpretation of the first term as a kind of modulation is facilitated by the application of a general formula (according to Huber) [23] enabling us to convert covariances into the difference in two variances:

$$(I_1, I_1 \cdot A') = \left[(I_1 + I_1 \cdot A', I_1 + I_1 \cdot A') - (I_1 - I_1 \cdot A', I_1 - I_1 \cdot A') \right] / 4. \qquad (34s)$$

(ii) Similarly for the acceptor, the 1st term on the right side of Eq. 32s is the modulation of the acceptor signal (I_a) by the transferred energy ($I_1 \cdot A'$), and the 2nd term is the moment of the transferred energy. (iii) Eq. 31s expresses the counterintuitive observation that the reduction in donor moment in general is not compensated by the increase in acceptor moment. The difference depends on α, and will be zero for a special α when

$$\alpha = S_2 \cdot (I_a, I_1 \cdot A') / (I_1, I_1 \cdot A'). \qquad (35s)$$

Eq. 31s also informs us that the difference between the changes of the donor and acceptor moments can be attributed to the different degree of modulations of the donor and acceptor signals caused by the transferred energy, and when this modulation is the same the difference cancels (Eq. 35s). Eq. 35s has an important practical consequence: α depends on the optical conditions of the measurement and can be changed with the optical conditions at custom. For α values fulfilling Eq. 35s

$$\alpha = \sqrt{(d_a'' - d_a') / (d - d')} \qquad (36s)$$

is also fulfilled. As to the sign of the difference in Eq. 31s, it can be either positive or negative, but when S_2 (the ratio of acceptor's excitabilities at the acceptor and donor excitation wavelength) is adjusted experimentally to zero, then the sign is definitely positive, meaning that the expression of Eq. 36s gives an under estimation for the real α in these cases. It is also can be seen, that for weak FRET processes (A'≈0) this difference can be taken as zero, and Eq. 36s approximately equals to the real α irrespective of the value of S_2. Changes of donor and acceptor moments can also be interpreted as corresponding changes in entropy or information content of the signals (according to Kullback) [24]. In the framework of the entropy interpretation, Eq. 31s means that the reduction in entropy of the donor signal is not compensated for by an equal increase of entropy of the acceptor signal, there is a net entropy production (2nd term in Eq. 31s) responsible for the mixing of transferred energy with the donor and acceptor signals (reminiscent of „mixing entropy" of thermodynamics).

Error estimation of α determined from the quadratic equation (Eq. 9)

Fig. 7s *Dependence of CV_α on CV_{S1} and CV_{S2}*. Error estimation has been done with the Gaussian law of error propagation based on Eqs. 9, 13, 14 in the main text. The error surface belongs to data of the 3rd row of Table 2, Part A: Alexa-Fluor 488-conjugated L368 "low" as donor+Alexa-Fluor 546-conjugated W6/32 as acceptor (α=0.135). According to Eq. 9 error of α can be decomposed to errors in the D, p and q quantities. While D does not depend on the S_1 and S_2 spillage factors, p and q do, as shown by Eqs. 13, 14. The effect of the S_3 factor has not been taken into account being this factor negligibly small in our case (S_3=1.5x10^{-4}). Coefficient of variation square of

α has been estimated with coefficient of variation squares for D, p and q based on Eq. 9:
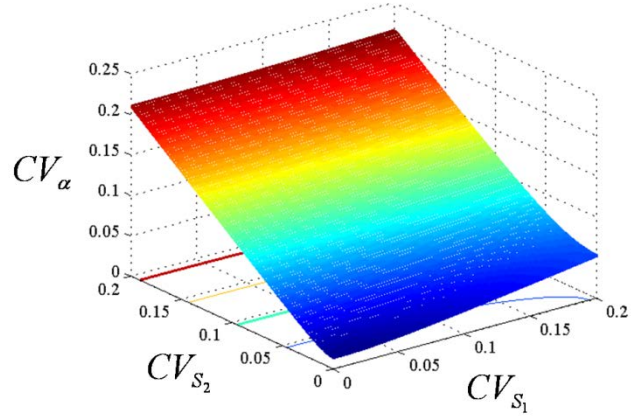
$$CV_\alpha^2 = \left[\tilde{p}^2 \cdot CV_p^2 + 1/4 \cdot \tilde{q}^2 \middle/ \left(\sqrt{\tilde{p}^2 + \tilde{q}} + \tilde{p} \right)^2 \cdot CV_q^2 \right] \middle/ \left(\tilde{p}^2 + \tilde{q} \right) + \left(2 \cdot p + q/\alpha \right)^2 \cdot CV_D^2, \tag{37s}$$

with $\tilde{p} \equiv p/D$, $\tilde{q} \equiv q/D$. Coefficient of variation squares for p and q has been computed based on Eqs. 13, 14:

$$CV_p^2 = \left(S_1^2 \cdot d'^2 \cdot CV_{S_1}^2 + S_2^2 \cdot d_{13}^2 \cdot CV_{S_2}^2 \right) \middle/ p^2, \tag{38s}$$

$$CV_q^2 = 4 \cdot \left[S_1^2 \cdot \left(S_1 \cdot d' + S_2 \cdot d_{13} - d_{12} \right)^2 \cdot CV_{S_1}^2 + S_2^2 \cdot \left(S_2 \cdot d_3 + S_1 \cdot d_{13} - d_{23} \right)^2 \cdot CV_{S_2}^2 \right] \middle/ q^2. \tag{39s}$$

With the definitions: $d' \equiv (I_1, I_1)$, $d_2 \equiv (I_2, I_2)$, $d_3 \equiv (I_3, I_3)$, $d_{ij} \equiv (I_i, I_j)$, i, j=1, 2, 3. Used constants: S_1=0.1143, S_2=0.096, D=1.2406 (D and d's are multiplied by 10^{-6}), p=0.04, q=0.01, d'=0.338, d_2=0.248, d_3=16.616, d_{12}=0.227, d_{13}=1.549. d_{23}=1.969, CV_D=0.1.

It can be seen from the error surface that at the experienced CV-s of the spillage factors (CV_{S1}=0.1095, CV_{S2}=0.0558) CV_α remains around 0.05.

Stability of α determined from the cubic equation (Eq. 20)

The sensitivity of the coefficients of the cubic equation Eq. 20 on changes in the S_1 and S_2 spillage factors has been examined by applying the Gaussian law of error propagation on the coefficients p_0, p_1, and p_2 (Eqs. 22-24, 40s-55s). (p_3 does not depend on S_1 and S_2.) These coefficients has been expressed as explicit functions of S_1 and S_2 based of the dependence of A', p, q on S_1 and S_2 as expressed by Eqs. 10s, 13, 14 (Eqs. 40s-55s). According to Figs. 8s-10s below, a 0.023 and 0.066 coefficients of variation of S_1 and S_2 cause 0.48, 0.28 and 0.2 coefficients of variation in p_0, p_1, and p_2, respectively. To see the degree of tolerance of α, a 10, 14, 24, and 10 %-change (the last three are half of those caused by the variation of S_1 and S_2) for each one of the p0-p3 coefficients, respectively – while the others has been kept constant – caused only a 4-13 % change in α. When all the 4 coefficients has been shifted by these %-values in either the increasing or the decreasing direction, only a ~10 % change in α could be elicited demonstrating a degree of resistance of α against changes in the coefficients p0-p3. Although these results have been obtained for the Alexa-Fluor 546-W6/32+Alexa-Fluor 647-W6/32 donor-acceptor pair, similar results could be calculated also for the L368-L368 mAb pair with the same dyes – the 7th row of Table 1 – and for the Alexa-Fluor 488-Alexa-Fluor 546 dye pair with both types of mAb – the 7th and 8th rows of Table 2.

Fig. 8s *Dependence of CV_{p0} on CV_{S1} and CV_{S2} (Eq. 53s).* The error surface has been calculated for the case of Alexa-Fluor 488-W6/32+Alexa-Fluor 546-W6/32 donor-acceptor pair – the 8th row of Table 1 – having parameter values: $\alpha_{cubic}=0.139$, $p_3=-19.574$, $p_2=-2.455$, $p_1=0.470$, $p_0=0.034$, $S_1=0.188$, $S_2=0.096$, $CV_{S1}=0.023$, $CV_{S2}=0.066$.
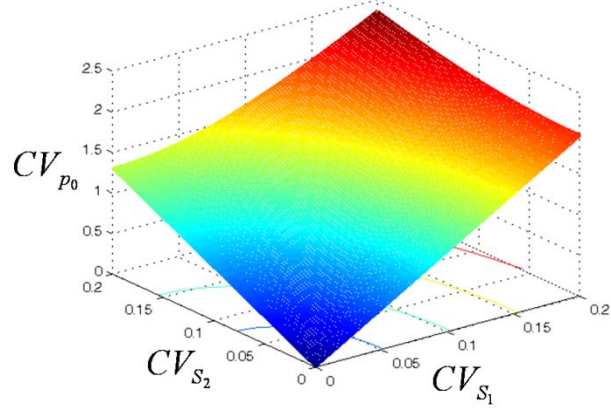
Fig. 9s *Dependence of CV_{p1} on CV_{S1} and CV_{S2} (Eq. 54s).* Sample and parameters are as above.
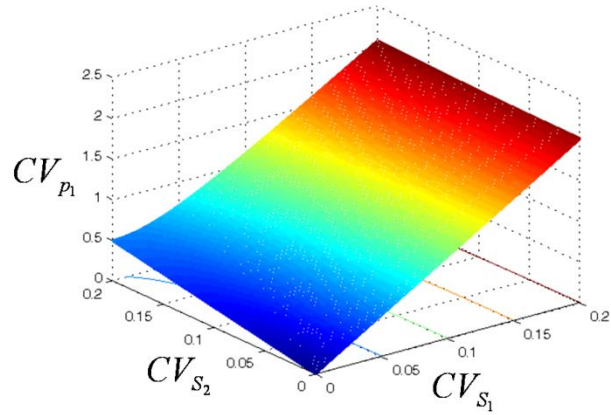
Fig. 10s *Dependence of CV_{p2} on CV_{S1} and CV_{S2} (Eq. 55s).* Sample and parameters are as above.
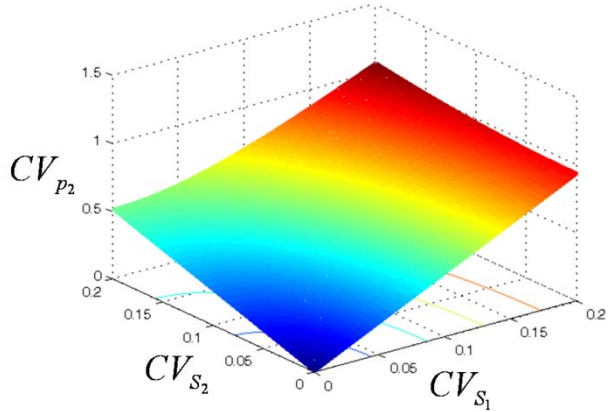
Formulae for the sensitivity of the cubic equation

For computing partial derivatives of the p_0, p_1, and p_2 according to the S_1 and S_2 spillage factors, first explicit forms of the p, q and A' quantities as functions of S_1 and S_2 are deduced from Eqs. 13, 14, and 10s:

$$p = d_{12} - S_1 \cdot d' - S_2 \cdot d_{13}, \tag{40s}$$

$$q = d_2 - 2 \cdot S_1 \cdot d_{12} - 2 \cdot S_2 \cdot d_{23} + 2 \cdot S_1 \cdot S_2 \cdot d_{13} + S_1^2 \cdot d' + S_2^2 \cdot d_3, \tag{41s}$$

$$A' = i_2 - S_2 \cdot i_3 - S_1, \tag{42s}$$

with the same definitions of the d-s as after Eq. 39s above, and with $i_2 = I_2/I_1$, and $i_3 = I_3/I_1$. According to Eqs. 22-24, the following partial derivatives are necessary for the calculation of errors: For p_0,

$$\partial A' q/\partial S_1 = -(2 \cdot i_2 \cdot d_{12} + d_2) + 2 \cdot S_1 \cdot (i_2 \cdot d' + 2 \cdot d_{12}) + 2 \cdot S_2 \cdot (i_2 \cdot d_{13} + i_3 \cdot d_{12} + d_{23}) \quad (43s)$$
$$- 2 \cdot S_1 \cdot S_2 (i_3 \cdot d' + 2 \cdot d_{13}) - 3 \cdot S_1^2 \cdot d' - S_2^2 \cdot (2 \cdot i_3 \cdot d_{13} + d_3),$$

$$\partial A' q/\partial S_2 = -(2 \cdot i_2 \cdot d_{23} + i_3 \cdot d_2) + 2 \cdot S_1 \cdot (i_2 \cdot d_{13} + i_3 \cdot d_{12} + d_{23}) + \quad (44s)$$
$$2 \cdot S_2 \cdot (i_2 \cdot d_3 + 2 \cdot i_3 \cdot d_{23}) - 2 \cdot S_1 \cdot S_2 (2 \cdot i_3 \cdot d_{13} + d_3) - S_1^2 \cdot (i_3 \cdot d' + 2 \cdot d_{13}) - 3 \cdot S_2^2 \cdot i_3 \cdot d_3.$$

For p_1:

$$\partial A' p/\partial S_1 = -(i_2 \cdot d' + d_{12}) + 2 \cdot S_1 \cdot d' + S_2 \cdot (i_3 \cdot d' + d_{13}), \quad (45s)$$

$$\partial A' p/\partial S_2 = -(i_2 \cdot d_{13} + i_3 \cdot d_{12}) + S_1 \cdot (i_3 \cdot d' + d_{13}) + 2 \cdot S_2 \cdot i_3 \cdot d_{13}, \quad (46s)$$

$$\partial q/\partial S_1 = -2 \cdot d_{12} + 2 \cdot S_1 \cdot d' + 2 \cdot S_2 \cdot d_{13}, \quad (47s)$$

$$\partial q/\partial S_2 = -2 \cdot d_{23} + 2 \cdot S_1 \cdot d_{13} + 2 \cdot S_2 \cdot d_3, \quad (48s)$$

$$\partial p_1/\partial S_1 = -2 \cdot (1 - m - b) \cdot \partial A' \cdot p/\partial S_1 - (1 - b) \cdot \partial q/\partial S_1, \quad (49s)$$

$$\partial p_1/\partial S_2 = -2 \cdot (1 - m - b) \cdot \partial A' \cdot p/\partial S_2 - (1 - b) \cdot \partial q/\partial S_2. \quad (50s)$$

For p_2:

$$\partial p_2/\partial S_1 = -(m - 2 + 3 \cdot b) \cdot d', \quad (51s)$$

$$\partial p_2/\partial S_2 = -(m + b) \cdot i_3 \cdot d' + 2 \cdot (1 - b) \cdot d_{13}. \quad (52s)$$

With these partial derivatives the CV^2-s are the following:

$$CV_{p_0}^2 = (1 - m - b) \cdot \left[(\partial A' q/\partial S_1)^2 \cdot S_1^2 \cdot CV_{S_1}^2 + (\partial A' q/\partial S_2)^2 \cdot S_2^2 \cdot CV_{S_2}^2 \right] / p_0^2, \quad (53s)$$

$$CV_{p_1}^2 = \left[(\partial p_1/\partial S_1)^2 \cdot S_1^2 \cdot CV_{S_1}^2 + (\partial p_1/\partial S_2)^2 \cdot S_2^2 \cdot CV_{S_2}^2 \right] / p_1^2, \quad (54s)$$

$$CV_{p_2}^2 = \left[(\partial p_2/\partial S_1)^2 \cdot S_1^2 \cdot CV_{S_1}^2 + (\partial p_2/\partial S_2)^2 \cdot S_2^2 \cdot CV_{S_2}^2 \right] / p_2^2. \quad (55s)$$

Supporting references

1. Hori, T., T. Uchiyama, M. Tsudo, H. Umadome, H. Ohno, S. Fukuhara, K. Kita, and H. Uchino. 1987. Establishment of an interleukin 2-dependent human T cell line from a patient with T cell chronic lymphocytic leukemia who is not infected with human T cell leukemia/lymphoma virus. *Blood* 70: 1069–1072.
2. Szöllősi, J., V. Hořejší, L. Bene, P. Angelisová, and S. Damjanovich. 1996. Supramolecular complexes of MHC class I, MHC class II, CD20, and tetraspan molecules (CD53, CD81, and CD82) at the surface of a B cell line JY. *J. Immunol.* 157: 2939-2946.

3. Tanabe, M., M. Sekimata, S. Ferrone, and M. Takiguchi. 1992. Structural and functional analysis of monomorphic determinants recognized by monoclonal antibodies reacting with HLA class I alpha 3 domain. *J. Immunol.* 148: 3202-3209.

4. Szöllősi, J., S. Damjanovich, M. Balázs, P. Nagy, L. Trón, M. J. Fulwyler, and F. M. Brodsky. 1989. Physical association between MHC class I and class II molecules detected on the cell surface by flow cytometric energy transfer. *J. Immunol.* 143: 208-213.

5. Edidin, M., and T. Wei. 1982. Lateral diffusion of H-2 antigens on mouse fibroblasts. *J. Cell Biol.* 95: 458-462.

6. Bene, L., M. Balázs, J. Matkó, J. Most, M. P. Dierich, J. Szöllősi, and S. Damjanovich. 1994. Lateral organization of the ICAM-1 molecule at the surface of human lymphoblasts: a possible model for its codistribution with the IL-2 receptor, class I and class II HLA molecules. *Eur. J. Immunol.* 24: 2115-2123.

7. Bacsó, Z., L. Bene, L. Damjanovich, and S. Damjanovich. 2002. IFN-γ rearranges membrane topography of MHC-I and ICAM-1 in colon carcinoma cells. *Biochem. Biophys. Res. Commun.* 290: 635-64.

8. Bene, L., Z. Kanyári, A. Bodnár, J. Kappelmayer, T. A. Waldmann, G. Vámosi, and L. Damjanovich. 2007. Colorectal carcinoma rearranges cell surface protein topology and density in CD4$^+$ T cells. *Biochem. Biophys. Res. Commun.* 361: 202-207.

9. Trón, L., J. Szöllősi , S. Damjanovich, S. H. Helliwell, D. J. Arndt-Jovin, and T. M. Jovin. 1984. Flow cytometric measurements of fluorescence resonance energy transfer on cell surfaces. Quantitative evaluation of the transfer efficiency on a cell-by-cell basis. *Biophys. J.* 45: 939-946.

10. Trón, L. 1994. Experimental methods to measure fluorescence resonance energy transfer. In: Mobility and proximity in biological membranes. S Damjanovich, J Szöllősi, L Trón, and M. Edidin, eds. CRC Press, Boca Raton, FL. p 1-47.

11. Szentesi, G., G. Horváth, I. Bori, G. Vámosi, J. Szöllősi, R. Gáspár, S. Damjanovich, A. Jenei, and L. Mátyus. 2004. Computer program for determining fluorescence resonance energy transfer efficiency from flow cytometric data on a cell-by-cell basis. *Comp. Meth. Prog. Biomed.* 75: 201-211.

12. Hanley, Q. S., V. Subramaniam, D. J. Arndt-Jovin, and T. M. Jovin. 2001. Fluorescence lifetime imaging: multi-point calibration, minimum resolvable differences, and artifact suppression. *Cytometry* 43: 248-260.

13. Esposito, A., H. C. Gerritsen, and F. S. Wouters. 2005. Fluorescence lifetime heterogeneity resolution in the frequency domain by lifetime moments analysis. *Biophys. J.* 89: 4286-4299.

14. Murphy, R. M., H. Slayter, P. Schurtenberger, R. A. Chamberlin, C. K. Colton, and M. L. Yarmush. 1988. Size and structure of antigen–antibody complexes. *Biophys. J.* 54:45–56.

15. Kerker, M., M. A. Van Dilla, A. Brunsting, J. P. Kratohvil, P. Hsu, D. S. Wang, J. W. Gray, and R. G. Langlois. 1982. Is the central dogma of flow cytometry true: that fluorescence intensity is proportional to cellular dye content? *Cytometry* 3/2: 71-78.

16. Hirschfeld, T. 1976. Quantum efficiency independence of the time integrated emission from a fluorescent molecule. *Applied optics* 15/12: 3135-3139.

17. Deka, C., B. E. Lehnert, N. M. Lehnert, G. M. Jones, L. A. Sklar, and J. A. Steinkamp. 1996. Analysis of fluorescence lifetime and quenching of FITC-conjugated antibodies on cells by phase-sensitive flow cytometry. *Cytometry* 25: 271-279.

18. MacDonald, R. I. 2006. Characteristics of self-quenching of the fluorescence of lipid-conjugated rhodamine in membranes. *J. Biol. Chem.* 1990; 265/23: 13533-13539.

19. Lakowicz, J. R. 2006. Fluorophores. Ch. 3 *In:* Principles of fluorescence spectroscopy. 3rd ed. Springer p 63-94.

20. Bojarski, C., and K. Sienicki. 1989. Energy transfer and migration in fluorescent solutions. Ch. 1 In: Photochemistry and photophysics, Vol. I. JF Rabek ed., CRC Press, Inc., p 1-56.

21. Bene, L., J. Szöllősi, G. Szentesi, L. Damjanovich, R. Jr. Gáspár, T. A. Waldmann, and S. Damjanovich. 2005. Detection of receptor trimers on the cell surface by flow cytometric fluorescence energy homotransfer measurements. *BBA Mol. Cell Res.* 1744: 176-198.

22. Rényi, A. 1981. Arbitrary random variables. Chapter IV *In:* Probability theory. 4th ed. Tankönyvkiadó, Budapest, p. 161-238.

23. Huber, P. J., and E. M. Ronchetti. 2009. Robust covariance and correlation matrices. Ch. 8. In: Robust statistics. 2nd ed. John Wiley & Sons Inc. p 199-237.

24. Kullback, S. 1997. Properties of information. Ch. 2. In: Information theory and statistics. Dover p 12-31.